AIDS RESEARCH AND HUMAN RETROVIRUSES
Volume 31, Number 7, 2015

DOI: 10.1089/aid.2015.0003

Increased Expression of CD169 on Blood Monocytes and Its Regulation by Virus and CD8 T Cells in Macaque Models of HIV Infection and AIDS

Woong-Ki Kim,[1] Christopher M. McGary,[1] Gerard E. Holder,[1] Adam R. Filipowicz,[1] Michael M. Kim,[1] Hind A. Beydoun,[2] Yanhui Cai,[3] Xianhong Liu,[4] Chie Sugimoto,[3] and Marcelo J. Kuroda[3]

Abstract

Increased expression of CD169 on monocytes has been reported in HIV-1-infected humans. Using rhesus macaque models of HIV infection, we sought to investigate whether simian immunodeficiency virus (SIV) infection upregulates CD169 expression on monocytes/macrophages. We also sought to determine whether CD8 T cells and plasma viral load directly impact the expression of CD169 on monocytes during SIV infection. We longitudinally assessed monocyte expression of CD169 during the course of SIV infection by flow cytometry, and examined the expression of CD169 on macrophages by immunohistochemistry in the spleen and lymph nodes of uninfected and infected macaques. CD169 expression on monocytes was substantially upregulated as early as 4 days during the hyperacute phase and peaked by 5–15 days after infection. After a transient decrease following the peak, its expression continued to increase during progression to AIDS. Monocyte CD169 expression was directly associated with plasma viral loads. To determine the contribution of $CD8^+$ T lymphocytes and virus to the control of monocyte CD169 expression, we used experimental $CD8^+$ lymphocyte depletion and antiretroviral therapy (ART) in SIV-infected macaques. Rapid depletion of CD8 T cells during acute infection of rhesus macaques induced an abrupt increase in CD169 expression. Importantly, levels of CD169 expression plummeted following initiation of ART and rebounded upon cessation of therapy. Taken together, our data reveal independent roles for virus and $CD8^+$ T lymphocytes in controlling monocyte CD169 expression, which may be an important link in further investigating the host response to viral infection.

Introduction

Monocytes/macrophages lie at the intersection of innate and adaptive immunity and are increasingly recognized for their role in the pathogenesis of HIV and the closely related simian immunodeficiency virus (SIV).[1–7] They are among the first cells to encounter foreign pathogens and initiate an immune response, and as a preferred target for HIV and SIV infection they are likely to provide a cellular source of viral reservoir that disseminates into anatomical sanctuaries, thus underscoring the importance of identifying indicators of early infection and activation in these cell types. Here we present CD169 as a useful monocyte marker to identify early viral infection and hypothesize its role in the activation of the adaptive immune response.

CD169 (sialoadhesin, Sn, or Siglec1) is a member of the sialic acid binding immunoglobulin-like lectins (SIGLECs) family.[8,9] This endocytic receptor binds and internalizes the sialylated bacteria and viruses. In addition, CD169 has been shown to mediate interactions with $CD8^+$ T lymphocytes and tumor cells via its counterreceptors CD43 and MUC1, respectively. While it was originally shown in mice that CD169 was expressed on specific subsets of tissue macrophages in secondary lymphoid organs such as the spleen and lymph nodes,[10] high CD169 expression has also been detected on blood monocytes from patients with systemic sclerosis,[11] systemic lupus erythematosus,[12] and primary biliary cirrhosis,[13] from patients undergoing acute hemodialysis,[14] and from pediatric intestinal transplant recipients who experienced acute cellular rejection.[15] Increased monocyte expression of CD169

[1]Department of Microbiology and Molecular Cell Biology and [2]Graduate Program in Public Health, Eastern Virginia Medical School, Norfolk, Virginia.
[3]Division of Immunology and [4]Division of Comparative Pathology, Tulane National Primate Research Center, Covington, Louisiana.

has also been reported in patients with viral infections such as Epstein–Barr virus enteritis[15] and HIV infection.[16–18] Upregulated expression of CD169 in monocytes in HIV-1-infected patients is associated with high viral loads, but not with low CD4 counts.[18] Interestingly, *in vitro* CD169 expression on monocytes is induced by antiviral interferon (IFN)-α and certain toll-like receptor ligands,[11,18] suggesting that type I IFN-mediated activation of monocytes may occur in HIV infection. Recently, it has been demonstrated that CD169 expressed on cultured monocytes and macrophages facilitated HIV-1 entry and *trans*-infection through interaction with the sialic acid residues on gp120 envelope glycoprotein.[18,19]

SIV infection of macaques has been widely used as the prime model for HIV/AIDS research since only macaques provide an animal model that recapitulates key features of human infection by HIV. In this longitudinal study, using SIVmac251-infected adult rhesus macaques, we investigated the kinetics of monocyte CD169 expression during SIV infection. Experimental $CD8^+$ lymphocyte depletion during the acute phase of infection and short-term antiretroviral therapy (ART) demonstrated roles for $CD8^+$ T lymphocytes and virus in modulating expression of CD169 on monocytes and possibly macrophages as well. In addition, we sought to investigate whether SIV infection affects the tissue-specific distribution or number of $CD169^+$ cells in the secondary lymphoid organs to propose a new role for $CD169^+$ macrophages in the immune response to HIV infection.

Materials and Methods

Animals

A total of 17 adult, male rhesus macaques (*Macaca mulatta*) were used in the study. All animals were housed at the Tulane National Primate Research Center (TNPRC). All procedures of this study were approved by the Tulane University Institutional Animal Care and Use Committee, and were carried out in accordance with the National Institutes of Health ''Guide for the Care and Use of Laboratory Animals'' and the recommendations of the Weatherall report, ''The use of non-human primates in research.'' All possible measures were taken to minimize discomfort of the animals. For all routine procedures such as blood collection and physical examination, animals were fully anesthetized with ketamine HCl under the direction of a veterinarian. Animals were humanely euthanized by the veterinary staff at the TNPRC in accordance with its endpoint policy. The criteria for euthanasia include 15% weight loss in 2 weeks, unresponsive opportunistic infection, persistent anorexia, severe intractable diarrhea, progressive neurological signs, significant cardiac and/or pulmonary signs, or any other serious illness. Euthanasia was conducted by anesthesia with ketamine HCl (10 mg/kg) followed by an overdose with sodium pentobarbital. This method is consistent with the recommendation of the American Veterinary Medical Association Guidelines on Euthanasia.

Fourteen animals were intravenously infected with 1 ml of 1000 $TCID_{50}$ SIVmac251. Archived tissues from three uninfected rhesus macaques were included as normal, uninfected controls. Blood was drawn at predetermined intervals, before and after infection, for complete blood count analysis and flow cytometry. Infected animals were euthanized when physiological signs of AIDS were observed. Necropsy specimens were collected in 10% neutral-buffered zinc formalin, embedded in paraffin, and sectioned at 5 μm. A list of infected animals can be found in Table 1.

Experimental $CD8^+$ lymphocyte depletion and ART

A total of 10 rhesus macaques received a depleting anti-CD8 antibody (clone M-T807R1; NIH Nonhuman Primate Reagent Resource) subcutaneously (sc) (10 mg/kg) at day 6 postinfection (pi) and intravenously (iv) (5 mg/kg) at days 8 and 12 pi. Among the 10 animals, four received a daily treatment of a nucleotide analog PMPA (20 mg/kg/day sc) and a nucleoside analog FTC (50 mg/kg/day sc) (Table 1). Unexpectedly, two of the four ART-treated animals died at 3 days after initiation of therapy due to ART-induced nephropathy.

Flow cytometric analysis of $CD169^+$ blood monocytes

Flow cytometry was performed as previously described.[4] EDTA-anticoagulated whole blood was stained and analyzed for $CD3^-CD8^-CD20^-HLA\text{-}DR^+CD14^+$ monocytes coexpressing CD16 or CD169 (phycoerythrin-conjugated antihuman CD169, clone 7-239; BioLegend, San Diego, CA) using FlowJo software (Tree Star, Ashland, OR). Previously, we tested another clone, HSn 7D2 (Santa Cruz Biotechnology, Santa Cruz, CA), and found it to cross-react to monkey monocytes as well. Controls were created using the appropriate isotype control (clone MOPC-21; BioLegend, San Diego, CA). Samples were run immediately on an 8-color BD FACSCalibur upgraded by Cytek Development (Fremont, CA). Monocytes were gated based on forward and side scatter profile and analyzed for the mean fluorescence intensity (MFI) of CD169 longitudinally over the course of SIV infection. The MFI was normalized to the isotype control for each time point to generate the arbitrary unit (AU) used for presentation of MFI data.

Immunohistochemistry for $CD169^+$ macrophages

Zinc formalin-fixed, paraffin-embedded tissues were assessed by immunohistochemistry, as previously described,[20] for the presence of CD169. Rabbit antihuman CD169 monoclonal antibody (clone SP213; Spring Bioscience, Pleasanton, CA) was used at a dilution of 1:500 in this study. Negative controls were prepared by omitting the primary antibody. After washing, sections were incubated for 30 min with a biotinylated secondary antibody, washed, and incubated with an avidin-biotin peroxidase complex (Vectastain ABC Elite kit: Vector Laboratories, Burlingame, CA) before development with diaminobenzidine (DAB) and counterstaining with hematoxylin for lymph node sections. For spleen section, alkaline phosphatase and its substrate NBT/BCIP were used instead to avoid nonspecific staining of red blood cells showing endogenous peroxidase activity. The spleen sections were counterstained with Vector Nuclear Fast Red. The stained sections were visualized using a Nikon Coolscope digital microscope (Melville, NY).

Determination of plasma viral load

The level of plasma viral RNA was quantified by the standard branched chain DNA amplification assay (Siemens Clinical Laboratory, Berkeley, CA). The limit of detection of viral RNA was 1,350 copies per milliliter of plasma.

Table 1. Animals Used in this Study

Group (size)	Animal number	Age (years)[a]	Time of survival (weeks)[b]	Period of cART[c]	Major clinical and pathological findings
Non-CD8 depleted ($n=4$)					
	GK40	5.02	27.1	None	*Klebsiella pneumoniae* pneumonia, lymphoid hyperplasia
	HA52	4.16	65.7	None	Mixed pattern of lymphoid hyperplasia and depletion, thymus atrophy
	IR99	5.30	69.3	None	Mild SIV encephalitis, multifocal, necrotic leukoencephalitis with intranuclear inclusions (SV40), lymphoid hyperplasia
	IT27	4.89	41.6	None	Malignant lymphoma, gastritis, enteropathy, interstitial pneumonia, lymphoid hyperplasia and dysplasia, thymus atrophy
CD8 depleted ($n=10$)					
	BK48	11.93	6.7	None	Lymphoid hyperplasia, neutrophilic neuritis with intranuclear CMV inclusions, mild SIV encephalitis
	CV39	10.31	21.0	None	Severe giant cell SIV encephalitis, mixed pattern of lymphoid hyperplasia and depletion
	DG09	10.02	14.0	None	Interstitial pneumonia, lymphoid depletion, thymus atrophy, mild SIV encephalitis, meningoencephalitis, myelitis
	DR28	8.53	16.3	None	Meningoencephalitis, interstitial pneumonia, lymphoid depletion
	DR67	9.03	7.0	None	Lymphoid hyperplasia
	EM89	8.27	10.0	Days 65–68[d]	ART nephropathy, giant cell pneumonia, edema, hypoproteinemia
	ER17	7.67	32.0	None	*Pneumocystis carinii* pneumonia, giant cell pneumonia, lymphoid hyperplasia and dysplasia, meningitis
	FI38	7.25	50.4	Days 65–116	Generalized amyloidosis, pneumonia with giant cells and intranuclear cytomegalovirus inclusions, mixed pattern of lymphoid hyperplasia and depletion
	GN17	5.23	70.4	Days 65–116	Meningitis, generalized lymphoid hyperplasia and dysplasia, thymus atrophy, giant cell colitis
	GN24	5.22	9.9	Days 65–68[d]	ART nephropathy, gastroenteritis, thymus atrophy, mild SIV encephalitis

[a]Indicates age at time of infection.
[b]Weeks after infection at time of euthanasia.
[c]PMPA and FTC were administered daily.
[d]Died unexpectedly of ART nephropathy.
cART, combination antiretroviral therapy; SIV, simian immunodeficiency virus; CMV, cytomegalovirus.

Statistical analysis

Statistical analyses were performed using SAS version 9.3. Two-sided statistical tests were conducted at an alpha level of 0.05. Group comparisons were performed using the Kruskal–Wallis test, with pairwise comparisons using Wilcoxon's rank sum test. Multivariate analyses were conducted using linear mixed-effects models.

Results

Monocyte expression of CD169 is rapidly increased during the preacute phase of SIV infection in rhesus macaques

Although increased monocyte expression of CD169 in SIV-infected rhesus macaques and HIV-1-infected humans was previously described,[17,18,21] the kinetics of monocyte CD169 expression during the course of HIV and SIV infection has not been well studied to date. To examine the effect of infection on CD169 expression by circulating monocytes in more detail, four adult rhesus macaques were infected with SIVmac251, and CD169 expression on *total* monocytes was monitored longitudinally by flow cytometry until euthanasia due to AIDS (Table 1 and Fig. 1A). Among blood cells, CD169 was found to be exclusively expressed on monocytes prior to and throughout the infection (data not shown). CD169 expression on the total monocyte population at baseline was low or negligible in all animals because the low expression of this molecule is restricted to minor subpopulations prior to infection (Fig. 2A). On day 4 after infection (the earliest time point pi), however, there was as much as a robust 10-fold increase in CD169 expression on monocytes. In all animals, CD169 expression on monocytes peaked at 5 to 15 days pi and then dropped slightly to a stable plateau. The absolute monocyte count did not change significantly during the same time period (data not shown). In three of four animals, a further increase in CD169 expression was seen within 3 to 4 months following the initial peak (Fig. 1A).

Since CD169 expression was markedly increased in blood monocytes early after SIV infection, we took a closer look at the relationship of CD169 expression to plasma viral load (PVL). The initial burst of plasma viral RNA levels following inoculation (at 12–18 days pi) corresponded temporally to the increase of CD169 expression on monocytes (Fig. 1B). PVL remained elevated thereafter for the entirety of infection except for one animal (monkey GK40), and high viral loads ($>100{,}000$ copies/ml) were associated with elevated monocyte expression of CD169. Interestingly, GK40, which died earlier at around week 27 pi, showed the corresponding drop in CD169 MFI and PVL in the final 2 weeks before death. In each animal, the rise and fall of viremia parallel the increase and decrease in CD169 expression during SIV infection. For analyses of the longitudinal data from the four animals, we used mixed effects models with day pi as a covariate. After

controlling for day pi, a statistically significant association was found between CD169 MFI and $\log_{10}$ PVL ($\beta = 259.05$, $p = 0.0032$). Results did not report statistically significant associations of CD169 MFI with CD4 count ($p = 0.1882$) or with CD8 count ($p = 0.0989$) (Fig. 1C and D).

$CD14^{++}CD16^{-}$ monocytes show a rapid increase in CD169 expression in response to SIV infection

Previously, we demonstrated, for the first time in nonhuman primates, the monocyte heterogeneity that underlies phenotypic changes in monocytes during SIV infection.[4] Here, we sought to investigate CD169 expression on different monocyte subsets before infection, in the acute and chronic phases of SIV infection (Fig. 2). Monocytes were gated based on forward and side scatter profile, differentiated based on the expression of CD14 and CD16 into $CD14^{high}16^{-}$, $CD14^{high}16^{low}$, and $CD14^{low}16^{high}$ subsets, and analyzed for the frequency of CD169-positive cells and normalized MFI of CD169 for each subset. Figure 2A shows representative CD14 versus CD16 bivariate contour plots of three selected time points before and during infection: preinfection (day 0 pi), acute (day 5 pi), and chronic (day 277 pi). While we observed the characteristic expansion of $CD14^{high}16^{low}$ monocytes during acute infection, it is the $CD14^{high}16^{-}$ population that had the greatest change in CD169 expression during this stage (Fig. 2A). A 2-log shift to the right in CD169 peak fluorescence channel within 5 days after SIV infection was observed only on $CD14^{high}16^{-}$ monocytes (depicted as a red line, Fig. 2A). The frequency of CD169-positive $CD14^{high}16^{-}$ monocytes increased from 9.7% to 70.2% during this early stage of acute infection ($p = 0.0304$, Wilcoxon's rank sum tests), which further increased up to 88.8% during chronic infection (Fig. 2B). Constitutive expression of CD169 on both $CD14^{high}16^{low}$ (green) and $CD14^{low}16^{high}$ (blue) monocytes increased more slowly over the course of infection (Fig. 2A). The frequencies of both subsets expressing CD169 were consistently greater than 80% (Fig. 2B). These results suggest that the MFI and percentage of CD169 expression on circulating monocytes, especially on the subset of $CD14^{high}16^{-}$ monocytes, may have the potential to be an *early* sensitive biomarker for SIV and HIV infection. Large-scale, future studies are needed to validate the utility of monocyte CD169 expression as an early biomarker of HIV/SIV infection.

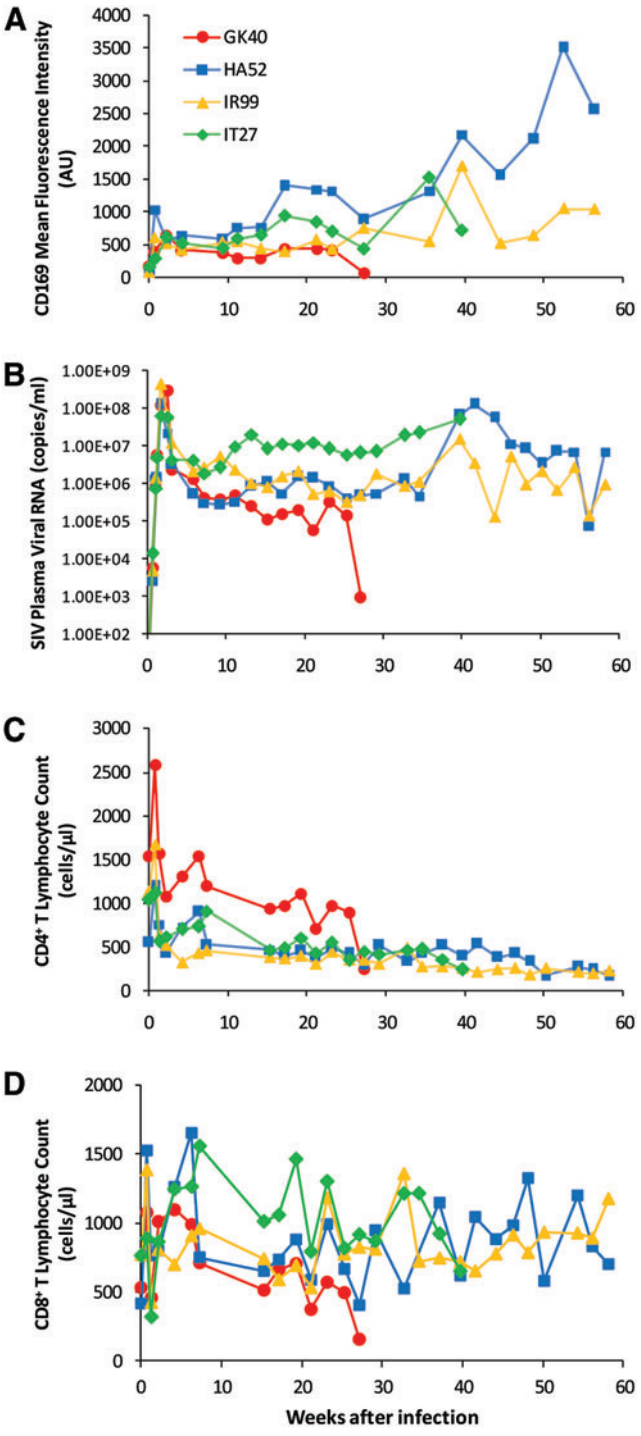

FIG. 1. Increased expression of CD169 on monocytes during the course of SIV infection. Four adult rhesus macaques were infected with SIVmac251. **(A)** Monocyte CD169 mean fluorescence intensities (arbitrary units, AU) measured by flow cytometry in individual macaques after infection are plotted over time. After being gated by their forward and side scatter properties, monocytes were further defined as $CD14^{+}$HLA-DR^{+} cells that are negative for CD3, CD8, and CD20. The mean fluorescence intensity of CD169 on total monocytes was normalized to the corresponding isotype control. **(B)** Plasma SIV viral loads in individual macaques after infection are shown. **(C)** Absolute counts of $CD4^{+}$ T lymphocytes and **(D)** absolute counts of $CD8^{+}$ T lymphocytes in individual macaques after infection are shown. Note: one animal (GK40) died early at around week 27 pi. Color images available online at www.liebertpub.com/aid

CD169 expression in macaque lymph nodes and spleen

In both humans and rodents, CD169 is expressed exclusively by specific subsets of macrophages in tissues. We used immunohistochemistry to examine the expression of CD169 in the spleen and lymph nodes of uninfected ($n = 3$) and SIV-infected ($n = 4$) rhesus macaques. Spleen sections were divided into anatomical regions and scored in a blind manner by a pathologist (X.L.) for $CD169^{+}$ cells (Table 2). In normal spleen, $CD169^{+}$ cells were found consistently in the germinal center, perifollicular zone, and red pulp (Fig. 3A). A few scattered $CD169^{+}$ cells were seen in the mantle zone, marginal zone, or periarteriolar lymphoid sheath (PALS). However, the

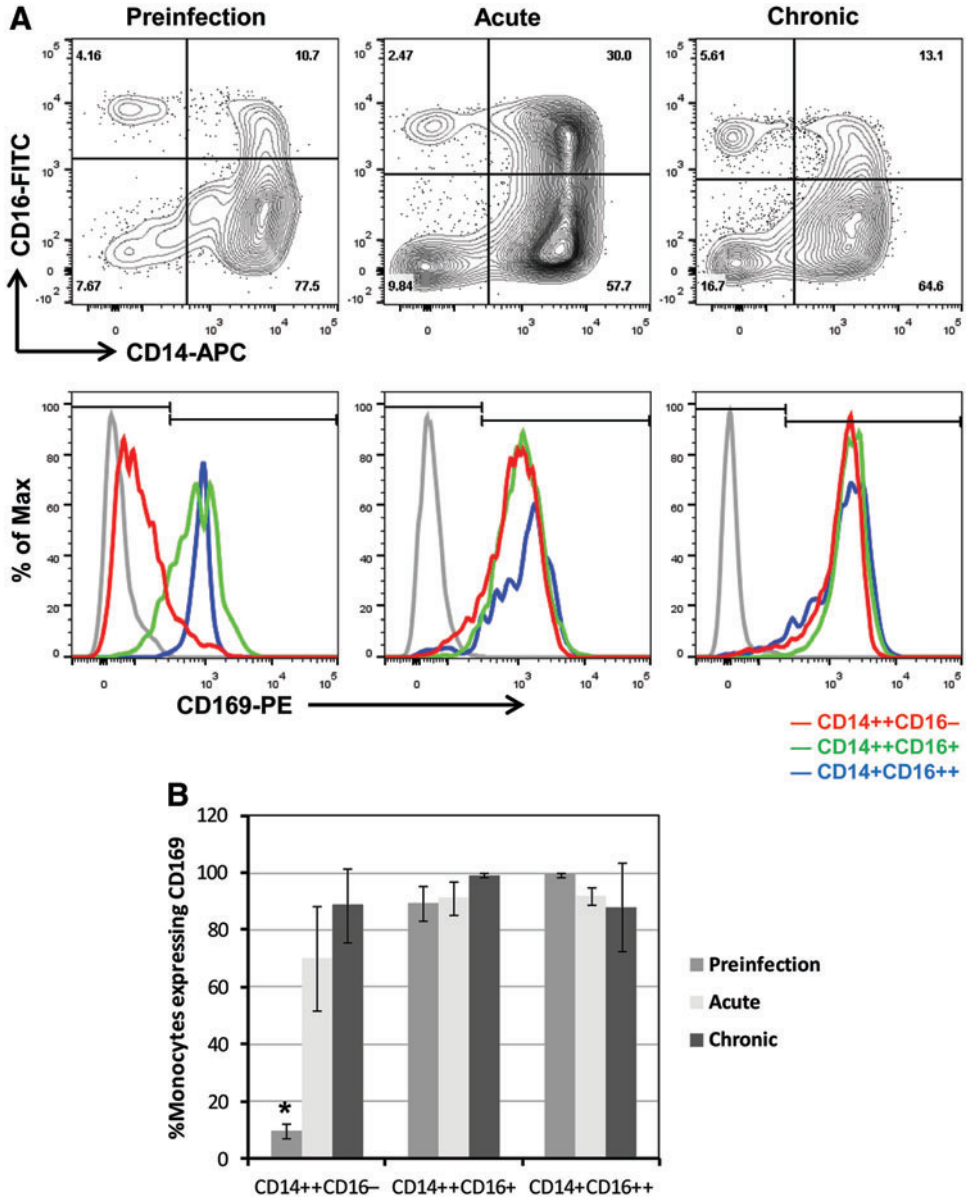

FIG. 2. Expression of CD169 on monocyte subsets in uninfected and SIV-infected macaques. **(A)** Using flow cytometry, we first gated on blood monocytes based on their forward versus side scatter properties, then excluded HLA-DR-negative cells and any cells that were positive for CD3, CD8, and CD20. Next, the blood monocytes were differentiated based on their expression of CD14 and CD16 **(A,** *top panels***)**. We examined the expression of CD169 on monocyte subsets including $CD14^{++}CD16^{-}$, $CD14^{++}CD16^{+}$, and $CD14^{+}CD16^{++}$ **(A,** *bottom panels***)**. Representative figures from preinfection (day 0 postinfection, *left panels*, $n=4$), acute infection (day 5 postinfection, *middle panels*, $n=4$), and chronic infection (day 277, *right panels*, $n=3$) are shown. *Gray*, isotype controls; *red*, CD169 expression on $CD14^{high}16^{-}$; *green*, $CD14^{high}16^{low}$; and *blue*, $CD14^{low}16^{high}$ subsets. The *y*-axis of the overlay histograms is not the number of cells but the percent of the maximum to depict the data in a normalized fashion. **(B)** The frequencies of CD169-positive cells in three different monocyte subsets before and after infection are plotted. Bars represent the mean and error bars represent the standard deviation. Kruskal–Wallis tests show that there is a significant difference in % $CD169^{+}$ monocytes between three time points during preinfection, acute and chronic infection within $CD14^{++}CD16^{-}$ ($p=0.0198$) and $CD14^{++}CD16^{+}$ ($p=0.0406$) subsets, but not within $CD14^{+}CD16^{++}$ ($p=0.0797$) subsets. For the $CD14^{++}CD16^{-}$ subset, we conducted a Wilcoxon's rank sum test to examine pairwise differences in % $CD169^{+}$ monocytes. We found a significant difference between preinfection and acute infection groups ($^{*}p=0.0304$). Differential expression of CD169 on monocyte subsets was confirmed in an additional six animals that were included in the $CD8^{+}$ cell depletion study (Table 1). Color images available online at www.liebertpub.com/aid

localization of $CD169^{+}$ cells in the spleen of SIV-infected rhesus macaques was different from normal uninfected macaques. As compared to normal uninfected animals, the marginal zone contained more $CD169^{+}$ macrophages and the red pulp had far fewer $CD169^{+}$ cells in SIV-infected animals (Fig. 3B). Overall, there appeared to be an increase in $CD169^{+}$ cell numbers in the white pulp, especially the marginal zone in SIV-infected animals.

We then examined the distribution and number of $CD169^{+}$ macrophages in the mesenteric, axillary, and inguinal lymph

TABLE 2. CD169 EXPRESSION ON MACROPHAGES IN THE SPLEEN OF UNINFECTED AND SIV-INFECTED RHESUS MACAQUES

Group (size)	*Animal number*	*Germinal center*	*Mantle zone*	*Marginal zone*	*Periarteriolar lymphoid sheath*	*Perifollicular zone*	*Red pulp*
Uninfected controls ($n=3$)							
	EC61	2	0	0	1	3	4
	GI53	2	0	0	1	3	4
	IT24	2	0	0	1	3	4
SIV infected ($n=4$)							
	GK40	1	1	2	1	2	2
	HA52	4	1	2	1	1	2
	IR99	1	3	1	1	2	2
	IT27	2	1	2	1	1	2

0, undetected; 1, minimal; 2, mild; 3, moderate; 4, strong.

nodes from uninfected and SIV-infected macaques. In uninfected macaques, $CD169^+$ macrophages were found in the subcapsular sinus, medullary sinus, and at the boundary between the cortical sinus and the paracortex (Fig. 3C). While the number of subcapsular sinus macrophages in the lymph nodes appeared not to be affected by SIV infection, strikingly there was a near-complete loss of $CD169^+$ cells or selective downregulation of CD169 on macrophages in the lymph node paracortex and medulla of all SIV-infected macaques (Fig. 3D). Interestingly, SIV-infected, $CD8^+$ lymphocyte-depleted macaques ($n=6$, see below for details) showed the retention of $CD169^+$ macrophages in the lymph node paracortex and medulla (Fig. 3E), suggesting that the loss of $CD169^+$ macrophages in the lymph nodes following SIV infection might be mediated by $CD8^+$ T lymphocytes.

A further accelerated rise in CD169 expression on monocytes is induced by $CD8^+$ lymphocyte depletion during acute SIV infection of rhesus macaques

To assess the role that CD8 T cells may play in regulating monocyte CD169 expression, we performed experimental *in vivo* $CD8^+$ lymphocyte depletion in rhesus macaques. A total of 10 SIVmac251-infected macaques received M-T807R1, a depleting anti-CD8 monoclonal antibody, at days 6, 8, and 12 pi (Table 1), a regimen previously shown to deplete $CD8^+$ lymphocytes in blood and lymph nodes for greater than 28 days.[22] CD8 T cells were depleted in all 10 monkeys in this study for 36 to 62 days, with no significant rebound observed in two of the 10 animals. In the remaining eight animals, CD8 T cell numbers rebounded partially but never fully recovered before euthanasia. Concomitant with the rapid disappearance of CD8 T cells at day 8 pi was a further dramatic increase in CD169 expression on monocytes, which occurred in all macaques receiving M-T807R1 antibody (Fig. 4). An abrupt increase of up to 99.3-fold in monocyte CD169 expression over preinfection levels peaked at 8 to 15 days pi. The CD169 MFI at the peaks are approximately 4- to 10-fold greater than in non-CD8-depleted animals. Based on linear mixed-effects model analyses, taking day pi as repeated measurements within each animal and CD8 depletion status as another covariate, the CD8-depleted group ($n=10$) has significantly higher CD169 expression than the non-CD8-depleted group ($n=4$) between 8 and 30 days pi ($\beta=2818$, $p=0.0008$).

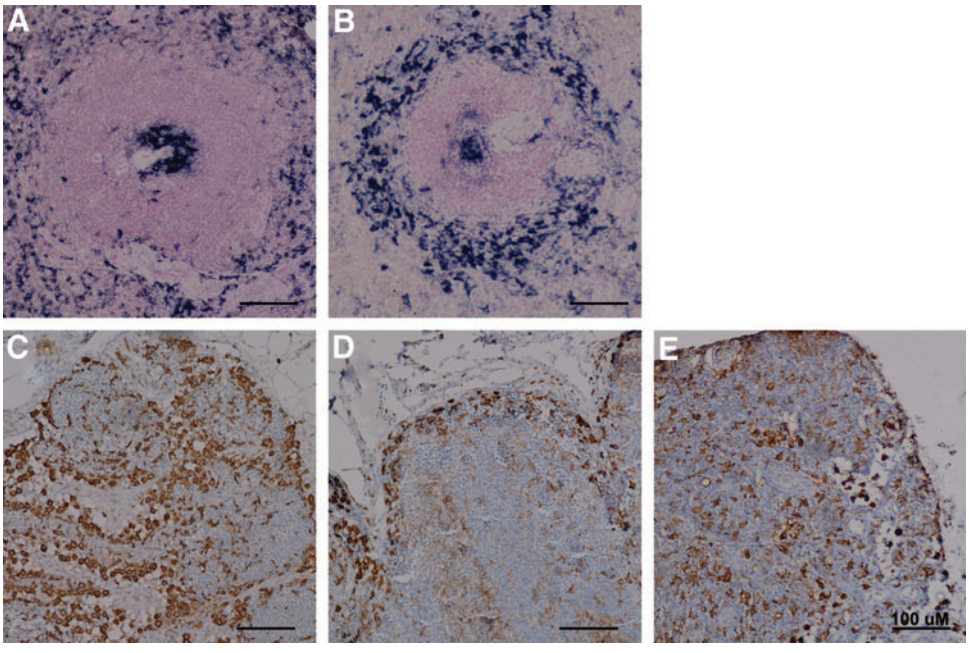

FIG. 3. Expression of CD169 in macaque lymph nodes and spleen. Representative images of $CD169^+$ tissue macrophages in uninfected and SIV-infected rhesus macaques. **(A, B)** Immunohistochemistry for CD169 (NBT-BCIP, *purple*) in spleen with hematoxylin counterstaining. **(C–E)** Immunohistochemistry for CD169 (DAB, *brown*) in lymph nodes with nuclear fast red counterstaining. *Left panels*, uninfected ($n=3$); *middle panels*, SIV-infected animals ($n=4$); *right panel*, SIV-infected, CD8-depleted animals ($n=6$). A minimum of two sections from mesenteric axillary and/or inguinal lymph nodes were stained for each animal. Color images available online at www.liebertpub.com/aid

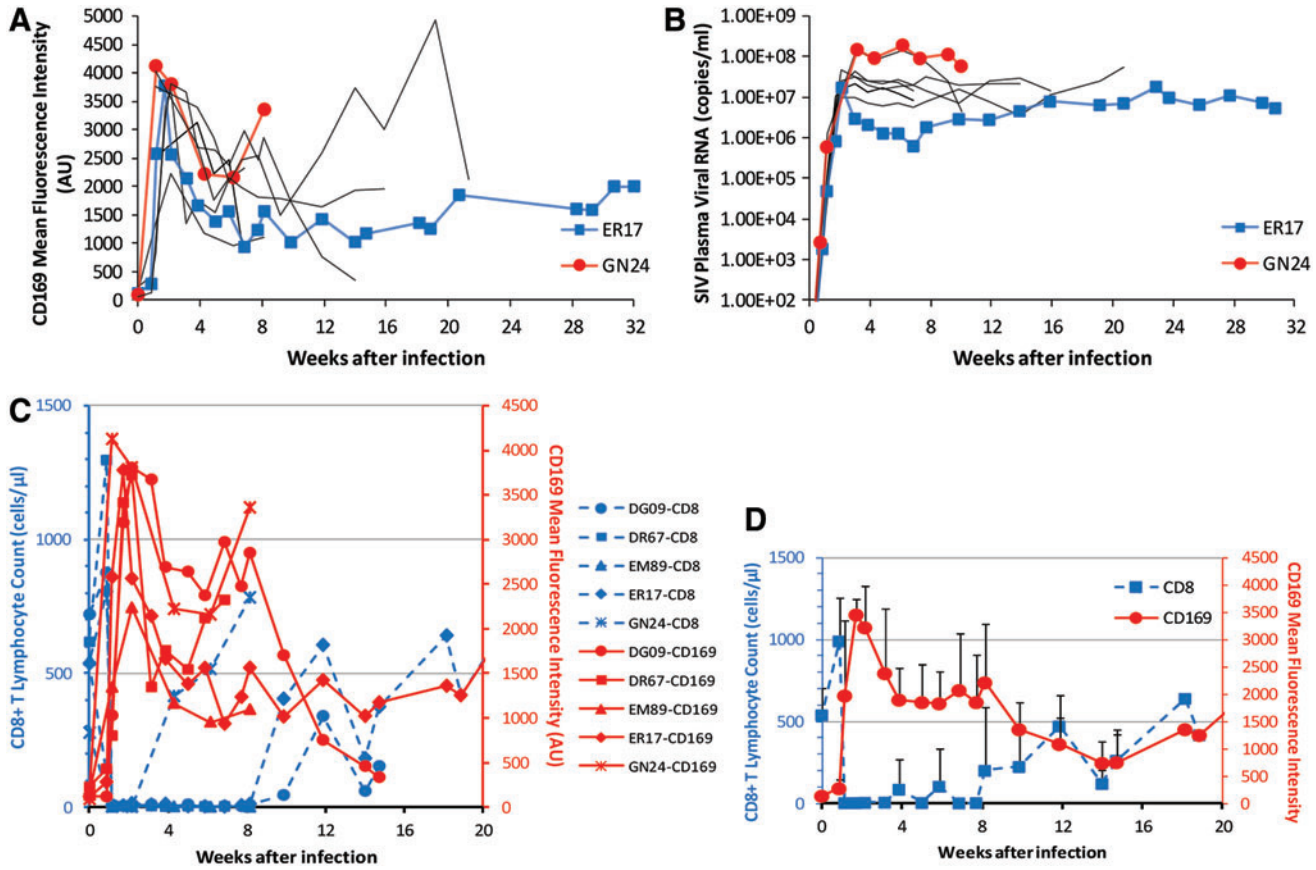

FIG. 4. Expression of CD169 on monocytes after CD8$^+$ lymphocyte depletion during acute SIV infection. Ten SIV-infected macaques were treated with anti-CD8 antibody M-T807R1 during acute infection. **(A)** Monocyte CD169 mean fluorescence intensities in individual macaques after infection are plotted over time. **(B)** Plasma SIV viral loads in individual macaques after infection are shown. One animal with a low viral load (ER17, *blue*) and one with a high viral load (GN24, *red*) are highlighted. **(C, D)** Temporal association between CD8 T cell count and monocyte CD169 expression. **(C)** Monocyte CD169 mean fluorescence intensities and CD8 counts in individual macaques after infection are plotted together. **(D)** Mean values of CD169 mean fluorescence intensities and CD8 counts are plotted. Color images available online at www.liebertpub.com/aid

Since previous data indicated that a statistically significant association existed between PVL and CD169 expression, we thought it was possible that the positive effect of CD8 T cell depletion on CD169 expression could be mediated indirectly through increased plasma viremia in these CD8-depleted animals. Thus, we examined PVL and CD169 MFI in detail during the first 2 weeks following anti-CD8 antibody treatment and during CD8$^+$ T lymphocyte rebound. There was no difference observed in peak levels of PVL during acute SIV viremia (at 12–22 days pi) between CD8$^+$ lymphocyte-depleted rhesus macaques and non-CD8-depleted controls ($1.0\times10^7-1.5\times10^8$ and $6.4\times10^7-4.6\times10^8$ copies/ml, respectively), as previously shown.[23] This showed that no further increase occurred in primary viremia owing to the CD8 depletion that could have accounted for the much higher expression levels of CD169 observed in CD8-depleted animals compared to non-CD8-depleted animals. We then looked closely at the association between PVL and CD169 expression during CD8 depletion ($n=10$). Using linear mixed-effects model analyses and taking day pi as repeated measurements within each animal, we found that no significant association exists between CD169 expression and PVL ($p=0.4977$) during early CD8 depletion (8–22 pi), while there was a significant association between CD169 MFI and $\log_{10}$ PVL ($\beta=468.64$, $p=0.0366$) for the entire period of SIV infection. Together, these data suggest that a further accelerated increase in viremia-driven CD169 expression during CD8 depletion could be induced by the absence of CD8 T cells during acute SIV infection.

Following acute peak viremia, CD8-depleted animals had no postpeak decline of viremia and had consistently higher PVL than nondepleted controls. After a peak, CD169 expression remained relatively high (higher than the peak levels in non-CD8-depleted animals) until the rebound of CD8$^+$ T lymphocytes. Figure 4A shows this trend among all the animals ($n=10$) we examined with two highlighted in particular, monkeys GN24 and ER17. GN24 and ER17 are the animals with high and low viral loads during the chronic phase of infection, respectively (Fig. 4B), which, in the SIV-infected, CD8$^+$ lymphocyte-depleted macaques, corresponded to relative CD169 expression levels the same as in the non-CD8-depleted animals.

Except for the animals that died early with no rebound of CD8 T cells, all the animals that were depleted of CD8 T cells showed rebound of CD8 T cells at different time points post-

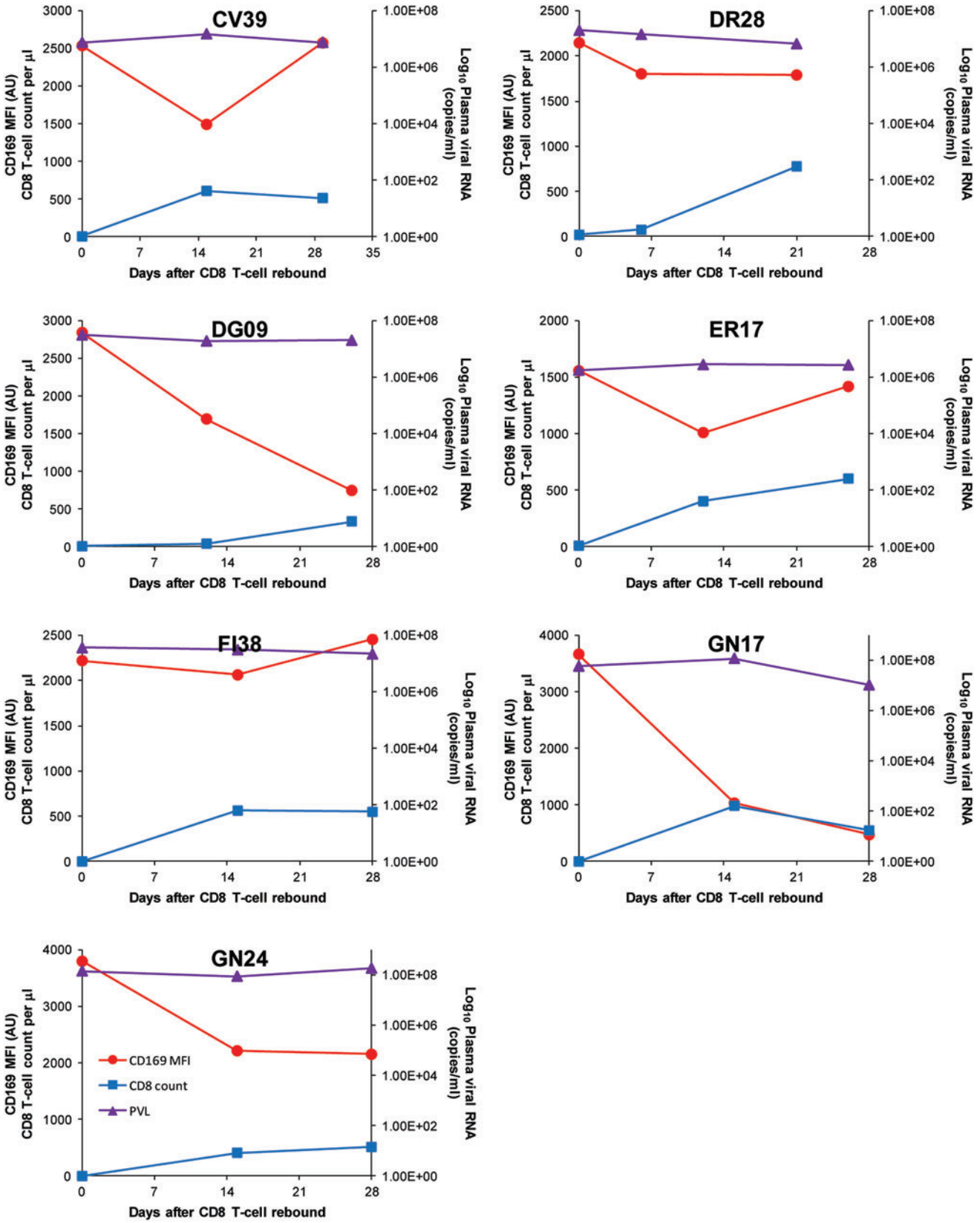

FIG. 5. Changes in CD169 expression levels, $CD8^+$ T lymphocyte count, and plasma viral loads during the rebound of CD8 T cells. Monocyte CD169 mean fluorescence intensities, plasma viral load, and CD8 counts are plotted together for each animal. $CD8^+$ T lymphocyte count, but not plasma viral load, is temporally associated with CD169 expression on blood monocytes during the rebound of CD8 T cells. Color images available online at www.liebertpub.com/aid

CD8 depletion (Fig. 4C). A dramatic decrease in CD169 expression was observed in all CD8-depleted animals at the time of the rebound of CD8 T cells. This temporal association can be seen more clearly in Fig. 4D, in which the decline of mean CD169 MFI and the rebound of mean CD8 T cell count of SIV-infected, CD8-depleted macaques were plotted together. Since a possible decrease in PVL during the CD8 rebound phase might have been responsible for the observed drop in CD169 expression, changes in PVL were plotted against the corresponding changes in absolute number of CD8 T cells and in CD169 MFI over the first month of CD8 rebound for each animal (Fig. 5). No decrease in PVL was found in association with CD8 rebound, and PVL did not temporally parallel CD169 MFI during CD8 rebound. On the other hand, the decrease in CD169 MFI was temporally associated with recovery of the $CD8^+$ T cell population in all macaques. These results suggest a possible role for CD8 T cells in controlling CD169 expression during HIV/SIV infection.

A profound decrease in CD169 expression following initiation of ART in SIV-infected, CD8-depleted macaques

To further examine the relation of CD169 expression to plasma virus and CD8 T cells, we sought to determine the effect of ART on monocyte CD169 expression in two SIV-infected, $CD8^+$ lymphocyte-depleted animals. As discussed in the previous section, the disappearance of CD8 T cells coincided with a further accelerated increase in CD169 expression on monocytes (Fig. 6A and C). Following administration of ART, expression levels of CD169 dropped to nearly zero (Fig. 6A). After ART was stopped, CD169 expression began to rebound to pretherapy levels. As expected, SIV plasma viral RNA levels also decreased upon initiation of therapy and increased after ART was discontinued (Fig. 6B). The drop and rebound of CD169 expression were temporally associated with the drop and rise of viremia in each animal. As found in the previous section, CD8 T cell recovery is accompanied by a dramatic decrease in CD169 expression. Thus, CD8 T cell recovery during ART could have a potential confounding effect on monocyte CD169 expression. However, when examining CD8 counts during ART we found that CD8 counts were not altered by ART (Fig. 6C). Therefore, the drop in CD169 expression was associated with a drop in viremia by ART without any confounding effect from CD8 T cell recovery. The mechanism for ART-mediated loss or downregulation of CD169 still remains to be determined. However, the temporal associations presented above suggest that ART decreases CD169 expression through viral suppression.

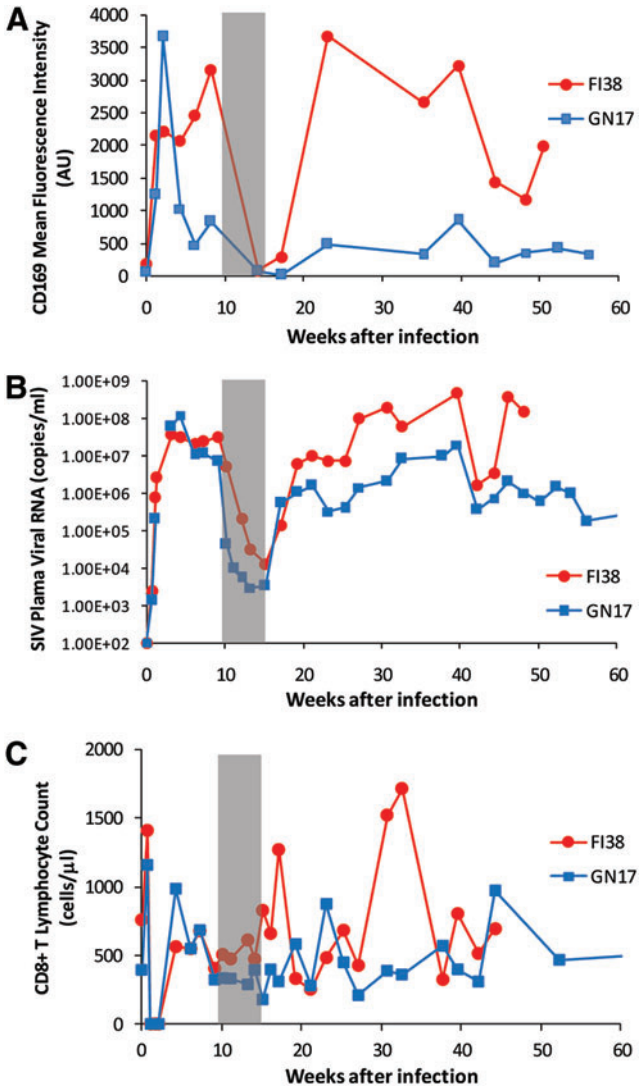

FIG. 6. Expression of CD169 on monocytes during and after antiretroviral therapy. Two SIV-infected macaques that were depleted of $CD8^+$ lymphocytes during acute infection received a short-term treatment of combination antiretroviral therapy (PMPA plus FTC). **(A)** Monocyte CD169 mean fluorescence intensities in individual macaques after infection are plotted over time. **(B)** Plasma SIV viral loads in individual macaques after infection are shown. **(C)** Absolute counts of $CD8^+$ T lymphocytes in individual macaques after infection are shown. The *gray shaded area* of each plot represents the period of antiretroviral therapy treatment. Color images available online at www.liebertpub.com/aid

Discussion

A biomarker that diagnoses early HIV infection before the virus was even detected in the blood or the one that predicts viral rebound after ART interruption would help HIV eradication efforts in the future. While further validation studies would need to be conducted in both macaques and humans, we took a first step, in this study, showing a potential utility of CD169 expression on monocytes, especially the $CD14^{high}CD16^-$ subset, as an early and highly sensitive biomarker of HIV/SIV infection. A profound decrease in CD169 MFI that was accompanied by suppressed viremia following combination ART provides further support for its utility. Using macaques depleted of $CD8^+$ lymphocytes *in vivo*, we were able to find temporal correlations that seem to suggest a possible role for $CD8^+$ T lymphocytes in suppressing the upregulation of monocyte CD169 expression in response to infection. We also examined the spleen and lymph nodes of uninfected and SIV-infected rhesus macaques for the presence of $CD169^+$ monocytes/macrophages and characterized changes in the distribution and number of $CD169^+$ macrophages in the spleen and lymph nodes of SIV-infected animals.

Recent data highlight the importance of $CD169^+$ macrophages in limiting the systemic dissemination of pathogens and activating CD8 T cells. Studies with vesicular stomatitis virus, vaccinia virus, and murine cytomegalovirus have demonstrated that $CD169^+$ subcapsular sinus and medullary macrophages in lymph nodes can capture and/or replicate viruses early after infection,[24–27] suggesting that pathogen capture by $CD169^+$ macrophages may be a generic host defense mechanism. $CD169^+$ macrophages have been implicated in the activation of $CD8^+$ T lymphocytes either by transferring the antigen to dendritic cells in the spleen[28] or by directly presenting antigen to $CD8^+$ T cells in draining lymph nodes.[29,30] Antigen cross-presentation by $CD169^+$ macrophages to CD8 T cells may be particularly important for immunity against HIV and SIV that does not readily infect monocytes/macrophages.

In this study, we found that the distribution of $CD169^+$ cells is altered during the course of SIV infection, which may indicate the important function of $CD169^+$ macrophages in HIV disease progression. With relevance to this, $CD169^+$ macrophages were shown to be targeted by activated CD8 T cells. This could be a mechanism to regulate the number of $CD169^+$ monocytes/macrophages or a way for pathogens to escape capture. $CD8^+$ T lymphocytes have been shown to mediate selective loss of marginal zone macrophages in the spleen after infection with lymphocytic choriomeningitis virus,[31] loss of splenic $CD169^+$ macrophages following *Plasmodium chabaudi* infection,[32] and loss of $CD169^+$ subcapsular sinus macrophages in the lymph nodes following *Toxoplasma gondii* infection.[29] Similarly, we observed a loss of $CD169^+$ medullary macrophage in the lymph nodes of SIV-infected rhesus macaques. Interestingly, in SIV-infected, CD8-depleted animals, the loss did not occur. Future investigation should further demonstrate the role of $CD169^+$ macrophages in HIV infection and provide insight into the application of targeting vaccines to $CD169^+$ macrophages to better elicit CD8 T lymphocyte responses.

Acknowledgments

This study was supported by grant funding from Virginia's Commonwealth Health Research Board to W.-K.K. (#11-09) and in part by Public Health Service Grants R21AI091501, R21AI110163, and R01AI097059 to M.J.K. We would like to thank Drs. Keith Reimann and Norman L. Letvin for the SIVmac251 stock that we used. We are also grateful to Drs. Joseph Mankowski, Cynthia Willard-Mack, and Marlon Rebelatto for discussions on the perifollicular zone of the monkey spleen. We are especially grateful to Dr. Edward M. Johnson who has read the manuscript and offered valuable comments.

Presented in part at the 32nd Annual Symposium on Nonhuman Primate Models for AIDS (NHP), November 11–14, 2014, Portland, Oregon (abstract P2.06).

Author Disclosure Statement

No competing financial interests exist.

References

1. Kim WK, Corey S, Alvarez X, and Williams K: Monocyte/macrophage traffic in HIV and SIV encephalitis. J Leukoc Biol 2003;74:650–656.
2. Hasegawa A, Liu H, Ling B, *et al.:* The level of monocyte turnover predicts disease progression in the macaque model of AIDS. Blood 2009;114(14):2917–2925.
3. Williams KC and Burdo TH: HIV and SIV infection: The role of cellular restriction and immune responses in viral replication and pathogenesis. APMIS 2009;117:400–412.
4. Kim WK, Sun Y, Do H, *et al.:* Monocyte heterogeneity underlying phenotypic changes in monocytes according to SIV disease stage. J Leukoc Biol 2010;87:557–567.
5. Kuroda MJ: Macrophages: Do they impact AIDS progression more than CD4 T cells? J Leukoc Biol 2010;87:569–573.
6. Centlivre M, Legrand N, Steingrover R, *et al.:* Altered dynamics and differential infection profiles of lymphoid and myeloid cell subsets during acute and chronic HIV-1 infection. J Leukoc Biol 2011;89:785–795.
7. Laforge M, Campillo-Gimenez L, Monceaux V, *et al.:* HIV/SIV infection primes monocytes and dendritic cells for apoptosis. PLoS Pathog 2011;7:e1002087.
8. Crocker PR, Hartnell A, Munday J, and Nath D: The potential role of sialoadhesin as a macrophage recognition molecule in health and disease. Glycoconj J 1997;14:601–609.
9. Klaas M and Crocker PR: Sialoadhesin in recognition of self and non-self. Semin Immunopathol 2012;34:353–364.
10. Crocker PR and Gordon S: Mouse macrophage hemagglutinin (sheep erythrocyte receptor) with specificity for sialylated glycoconjugates characterized by a monoclonal antibody. J Exp Med 1989;169:1333–1346.
11. York MR, Nagai T, Mangini AJ, *et al.:* A macrophage marker, Siglec-1, is increased on circulating monocytes in patients with systemic sclerosis and induced by type I interferons and toll-like receptor agonists. Arthritis Rheum 2007;56:1010–1020.
12. Biesen R, Demir C, Barkhudarova F, *et al.:* Sialic acid-binding Ig-like lectin 1 expression in inflammatory and resident monocytes is a potential biomarker for monitoring disease activity and success of therapy in systemic lupus erythematosus. Arthritis Rheum 2008;58:1136–1145.
13. Bao G, Han Z, Yan Z, *et al.:* Increased Siglec-1 expression in monocytes of patients with primary biliary cirrhosis. Immunol Invest 2010;39:645–660.
14. Ramirez R, Carracedo J, Berdud I, *et al.:* Microinflammation in hemodialysis is related to a preactivated subset of monocytes. Hemodial Int 2006;10(Suppl 1):S24–S27.
15. Ashokkumar C, Gabriellan A, Ningappa M, *et al.:* Increased monocyte expression of sialoadhesin during acute cellular rejection and other enteritides after intestine transplantation in children. Transplantation 2012;93:561–564.
16. Pulliam L, Sun B, and Rempel H: Invasive chronic inflammatory monocyte phenotype in subjects with high HIV-1 viral load. J Neuroimmunol 2004;157:93–98.
17. van der Kuyl AC, van den BR, Zorgdrager F, *et al.:* Sialoadhesin (CD169) expression in CD14+ cells is upregulated early after HIV-1 infection and increases during disease progression. PLoS One 2007;2:e257.
18. Rempel H, Calosing C, Sun B, and Pulliam L: Sialoadhesin expressed on IFN-induced monocytes binds HIV-1 and enhances infectivity. PLoS One 2008;3:e1967.
19. Zou Z, Chastain A, Moir S, *et al.:* Siglecs facilitate HIV-1 infection of macrophages through adhesion with viral sialic acids. PLoS One 2011;6:e24559.
20. Kim WK, Alvarez X, Fisher J, *et al.:* CD163 identifies perivascular macrophages in normal and viral encephalitic brains and potential precursors to perivascular macrophages in blood. Am J Pathol 2006;168:822–834.

21. Jaroenpool J, Rogers KA, Pattanapanyasat K, *et al.:* Differences in the constitutive and SIV infection induced expression of Siglecs by hematopoietic cells from non-human primates. Cell Immunol 2007;250:91–104.
22. Williams K and Burdo TH: Monocyte mobilization, activation markers, and unique macrophage populations in the brain: Observations from SIV infected monkeys are informative with regard to pathogenic mechanisms of HIV infection in humans. J Neuroimmune Pharmacol 2012;7:363–371.
23. Schmitz JE, Kuroda MJ, Santra S, *et al.:* Control of viremia in simian immunodeficiency virus infection by CD8+ lymphocytes. Science 1999;283:857–860.
24. Junt T, Moseman EA, Iannacone M, *et al.:* Subcapsular sinus macrophages in lymph nodes clear lymph-borne viruses and present them to antiviral B cells. Nature 2007; 450:110–114.
25. Hsu KM, Pratt JR, Akers WJ, *et al.:* Murine cytomegalovirus displays selective infection of cells within hours after systemic administration. J Gen Virol 2009;90:33–43.
26. Iannacone M, Moseman EA, Tonti E, *et al.:* Subcapsular sinus macrophages prevent CNS invasion on peripheral infection with a neurotropic virus. Nature 2010;465:1079–1083.
27. Hickman HD, Li L, Reynoso GV, *et al.:* Chemokines control naive CD8+ T cell selection of optimal lymph node antigen presenting cells. J Exp Med 2011;208:2511–2524.
28. Backer R, Schwandt T, Greuter M, *et al.:* Effective collaboration between marginal metallophilic macrophages and CD8+ dendritic cells in the generation of cytotoxic T cells. Proc Natl Acad Sci USA 2010;107:216–221.
29. Chtanova T, Han SJ, Schaeffer M, *et al.:* Dynamics of T cell, antigen-presenting cell, and pathogen interactions during recall responses in the lymph node. Immunity 2009; 31:342–355.
30. Asano K, Nabeyama A, Miyake Y, *et al.:* CD169-positive macrophages dominate antitumor immunity by cross-presenting dead cell-associated antigens. Immunity 2011; 34:85–95.
31. Odermatt B, Eppler M, Leist TP, *et al.:* Virus-triggered acquired immunodeficiency by cytotoxic T-cell-dependent destruction of antigen-presenting cells and lymph follicle structure. Proc Natl Acad Sci USA 1991;88:8252–8256.
32. Beattie L, Engwerda CR, Wykes M, and Good MF: CD8+ T lymphocyte-mediated loss of marginal metallophilic macrophages following infection with Plasmodium chabaudi chabaudi AS. J Immunol 2006;177:2518–2526.

Address correspondence to:
Woong-Ki Kim
Department of Microbiology and Molecular Cell Biology
Eastern Virginia Medical School
700 West Olney Road
Lewis Hall 3174
Norfolk, Virginia 23507

E-mail: kimw@evms.edu